Why does Steady-State Magnetic Reconnection have a Maximum Local Rate of Order 0.1?

Yi-Hsin Liu,[1] M. Hesse,[1] F. Guo,[2] W. Daughton,[2] H. Li,[2] P. A. Cassak,[3] and M. A. Shay[4]
[1]NASA-Goddard Space Flight Center, Greenbelt, Maryland 20771, USA
[2]Los Alamos National Laboratory, Los Alamos, New Mexico 87545, USA
[3]West Virginia University, Morgantown, West Virginia 26506, USA
[4]University of Delaware, Newark, Delaware 19716, USA

(Received 17 August 2016; revised manuscript received 24 October 2016; published 21 February 2017)

Simulations suggest collisionless steady-state magnetic reconnection of Harris-type current sheets proceeds with a rate of order 0.1, independent of dissipation mechanism. We argue this long-standing puzzle is a result of constraints at the magnetohydrodynamic (MHD) scale. We predict the reconnection rate as a function of the opening angle made by the upstream magnetic fields, finding a maximum reconnection rate close to 0.2. The predictions compare favorably to particle-in-cell simulations of relativistic electron-positron and nonrelativistic electron-proton reconnection. The fact that simulated reconnection rates are close to the predicted maximum suggests reconnection proceeds near the most efficient state allowed at the MHD scale. The rate near the maximum is relatively insensitive to the opening angle, potentially explaining why reconnection has a similar fast rate in differing models.

DOI: 10.1103/PhysRevLett.118.085101

Introduction.—A significant amount of magnetic energy is released in solar and stellar flares [1–3], substorms in magnetotails of Earth and other planets [4,5], disruptions and the sawtooth crash in magnetically confined fusion devices [6], laboratory experiments [7], and numerous high energy astrophysical systems [8,9]. Magnetic reconnection, where a change in topology of the magnetic field allows a rapid release of magnetic energy into thermal and kinetic energy, is a likely cause. The reconnection electric field parallel to the X line (where magnetic field lines break) not only determines the rate that reconnection proceeds, but can also be crucial for accelerating energetic superthermal particles. It was estimated that a normalized reconnection rate of $\simeq 0.1$ is required to explain the time scales of flares and substorms [10].

Reconnection rates have been studied observationally, experimentally, theoretically, and numerically. Measurements can be *in situ*, such as in the magnetosphere and lab, or remote, as in solar and astrophysical contexts. Reconnection rates from these different vantage points can be the same but need not be; for example, flux ropes in the corona have macroscopic forces that can influence the evolution of current sheets where reconnection occurs. Therefore, it is important to distinguish between system scales. We define *global* scale as system-size scale of magnetic domains. The *local* scale is a smaller MHD-scale region where the magnetic field and plasma parameters achieve relatively uniform conditions upstream of the diffusion region. The *microscale* is the scale of the diffusion region, which for collisionless reconnection is the ion diffusion region and below. Here we focus on reconnection rates at the local- and microscales; coupling to global scales is beyond the scope of this Letter.

The original model for the local reconnection rate was the Sweet-Parker model [11,12], but it was too slow to explain observed time scales of flares and substorms [13]. The collisional diffusion region is long and thin (i.e., the upstream magnetic fields have a small opening angle), developing a bottleneck that keeps the inflow speed small. The Petschek model [14] was much faster because it had an open outflow region (i.e., a larger opening angle), but is not a self-consistent model [15,16].

The collisionless limit is more appropriate for many systems of interest. Two-dimensional (2D) local simulations of isolated, thin, Harris-type current sheets reveal that the steady-state reconnection has a fast rate of 0.1 [17] when normalized by the magnetic field and Alfvén speed at the local scale. This rate is independent of simulated electron mass [18,19] and system size [17,19]. In particular, the GEM challenge study [20] showed that the rate is comparable in Hall-MHD, hybrid, and particle-in-cell (PIC) simulations. Consequently, it was argued that the Hall term, the minimal non-ideal-MHD term in all three models, is the key physics for producing the fast rate [21,22]. However, further studies have raised important questions. One gets similar fast rates in electron-positron plasmas, for which the Hall term vanishes [23–25], and in the strong out-of-plane (guide) magnetic field regime [26–29] for which the Hall term is inactive. Even within resistive MHD, the same 0.1 rate arises when a localized resistivity is employed [16]. This evidence calls into question whether the Hall term is the critical effect. It was suggested that the appearance of secondary islands could provide a universal mechanism for limiting the length of the diffusion region [24,26], but this model is also not

satisfying since the same rate is obtained even when islands are absent [22,30].

In situ magnetospheric observations reveal (local) reconnection rates near 0.1 [31,32]. Solar observations suggest (global) reconnection rates can be this high as well [33–35], or somewhat lower [36,37]. Therefore, observations suggest the local rate is 0.1, and the global rate can be at or below 0.1. This also has numerical support; in island coalescence, the global rate can be lower than 0.1 [38–40], while the local rate remains close to 0.1 [38].

What causes the local reconnection rate to be ~0.1 across different systems remains an open question [e.g., Ref. [41]]. In this Letter, we offer a new approach to this long-standing problem. We propose that the local rate has a maximum as a result of constraints at MHD scales (rather than physics at the diffusion-region scale as is typically discussed). We perform an analysis to derive the maximum local rate for low-β plasmas, which we find is $O(0.1)$. The fact that local simulations produce rates close to this maximum value suggests that steady reconnection proceeds at a rate nearly as fast as possible. We show the predictions are consistent with PIC simulations of a relativistic electron-positron plasma and a nonrelativistic electron-proton plasma. In this study, we restrict our attention to antiparallel reconnection for simplicity.

Simple model.—Let the thickness and length of the (microscale) diffusion region be δ and L, respectively. For collisionless reconnection, δ is controlled by inertial or gyroradius scales [42]. If the opening angle made by the upstream magnetic field is small, the diffusion region is long and thin. Reconnection in this case is very slow, as in Sweet-Parker reconnection [11,12]. As the opening angle increases, reconnection becomes faster. This is true to a point, but cannot continue for all angles for two reasons. First, in order to satisfy force balance, the upstream region develops structures over a larger scale, as in the classical Petschek-type analyses [14,43]; this is what we define as the local scale. Since the diffusion region thickness continues to be controlled by microscales, the diffusion region becomes embedded in a wider structure [42,44,45] of local scale Δz, where the magnetic field and plasma parameters achieve relatively uniform upstream conditions. The magnetic field B_{xm} immediately upstream of the diffusion region becomes smaller than the asymptotic magnetic field B_{x0}. (The subscript 0 indicates asymptotic quantities at the local scale and m indicates quantities at the microscale.) This is crucial because it is B_{xm} that drives the outflow from the diffusion region; as it becomes smaller, reconnection proceeds more slowly.

The second reason reconnection does not become faster without bound is that the $\mathbf{J}\times\mathbf{B}$ force of the reconnected field becomes smaller as the opening angle increases [46]. In the limit where the separatrices are at a right angle, the tension force driving the outflow is canceled by the magnetic pressure force, so reconnection does not occur.

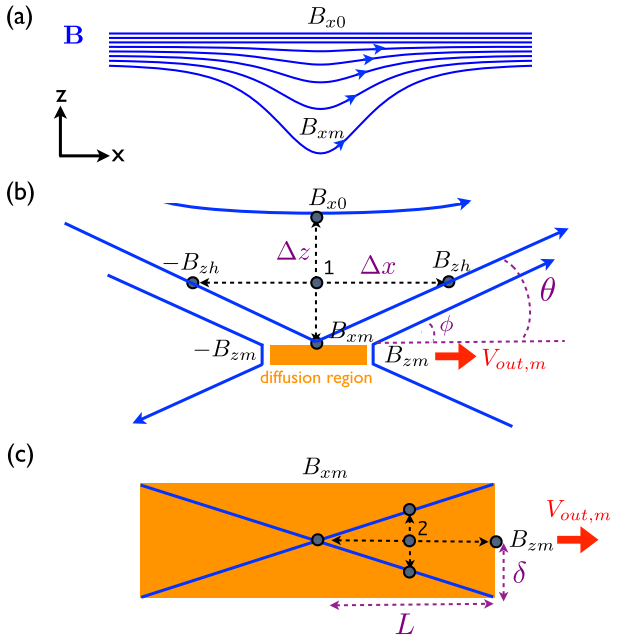

FIG. 1. (a) Sketch of magnetic field lines upstream of the diffusion region ($z > 0$). (b) Geometry of reconnection at the local scale. (c) Dimensions of the diffusion region at the microscale.

These observations suggest the following: the reconnection rate has a maximal value for an intermediate opening angle which is large enough to avoid the bottleneck for extremely thin current layers, but is not too large to weaken the reconnection drive. We present an analysis simply capturing these main aspects using only the reconnection geometry and force balance. We consider low-β systems in the relativistic limit; a more general derivation should be considered in future work.

The inflow region is illustrated in Fig. 1(a). With the diffusion region at the microscale, the asymptotic (local) magnetic field (at the top) must bend as it weakens toward the diffusion region (at the bottom). In the $\beta \ll 1$ limit, thermal pressure is negligible, so to remain near equilibrium the inward-directed magnetic pressure gradient force $-(\nabla B^2/8\pi)_z$ must be almost perfectly balanced by outward-directed magnetic tension $\mathbf{B}\cdot\nabla B_z/4\pi$. Evaluating these at point 1 marked in Fig. 1(b) gives

$$\frac{B_{x0}^2 - B_{xm}^2}{8\pi\Delta z} \simeq \left(\frac{B_{x0}+B_{xm}}{2}\right)\frac{2B_{zh}}{4\pi\Delta x}, \tag{1}$$

where B_{zh} is evaluated at the upstream field line near the separatrix. (Note that the inertia of the inflowing plasmas can be included in Eq. (1) using $V_z = cE_y/B_x$, but its effect is negligible.)

We make the reasonable assumption the opening angle made by the upstream field at the local scale, $\theta \equiv \tan^{-1}(\Delta z/\Delta x)$, matches the opening angle of the microscale field at the corner of the ion diffusion region, $\phi \equiv \tan^{-1}(B_{zm}/B_{xm})$. Then, from geometry, we get

$B_{zh}/[(B_{x0}+B_{xm})/2] \simeq \Delta z/\Delta x \simeq B_{zm}/B_{xm}$. Eliminating B_{zh} and solving for B_{xm}/B_{x0} gives

$$\frac{B_{xm}}{B_{x0}} \simeq \frac{1-(\Delta z/\Delta x)^2}{1+(\Delta z/\Delta x)^2}. \quad (2)$$

For small opening angles, $B_{xm} \simeq B_{x0}$; for large opening angles approaching 45°, $B_{xm} \ll B_{x0}$, and embedding is significant.

To estimate the outflow speed, we employ force balance in the x direction at point 2 in Fig. 1(c). In the relativistic limit [47], $n' m_i U_{\rm out}^2/2L + B_{zm}^2/8\pi L \simeq (B_{zm}/2)2(B_{xm}/2)/4\pi\delta$, where n' is the density measured in the fluid rest frame, m_i is the ion mass, $U_{\rm out}$ is the x component of the 4-velocity. Note that we have assumed that the profile of plasma pressure in the outflow direction is nearly uniform, as has been done in previous analyses [48], so that the pressure gradient force is small compared to the magnetic tension force. The outflow speed $V_{{\rm out},m}$ from the end of the diffusion region is related to $U_{\rm out}$ through $U_{\rm out} = \gamma_{\rm out} V_{{\rm out},m} = V_{{\rm out},m}/(1-V_{{\rm out},m}^2/c^2)^{1/2}$, where $\gamma_{\rm out}$ is the relativistic factor. Since the separatrix goes through the corner of the diffusion region, $B_{zm}/B_{xm} \simeq \delta/L$. Solving for the outflow speed as a function of δ/L gives

$$V_{{\rm out},m} \simeq c\sqrt{\frac{(1-\delta^2/L^2)\sigma_{xm}}{1+(1-\delta^2/L^2)\sigma_{xm}}}, \quad (3)$$

where the magnetization parameter evaluated near the diffusion region is $\sigma_{xm} = B_{xm}^2/4\pi n' m_i c^2$. Consequently, if $\delta/L \ll 1$, then $V_{{\rm out},m} \sim V_{Am}$ as expected since the Alfvén speed in the relativistic limit [49] is $V_{Am} = c[\sigma_{xm}/(1+\sigma_{xm})]^{0.5}$. However, as $\delta/L \to 1$, the outflow speed $\to 0$ [46].

Putting the results together yields a prediction for the normalized local rate. The reconnection electric field E_y is $B_{zm} V_{{\rm out},m}/c$. The reconnection rate $R_0 \equiv cE_y/B_{x0}V_{A0}$ normalized to local quantities is

$$R_0 \simeq \left(\frac{B_{zm}}{B_{xm}}\right)\left(\frac{B_{xm}}{B_{x0}}\right)\left(\frac{V_{{\rm out},m}}{V_{A0}}\right). \quad (4)$$

The rate normalized to the microscale magnetic field and Alfvén speed is $R_m \simeq (B_{zm}/B_{xm})(V_{{\rm out},m}/V_{Am})$, and the microscale inflow speed is $V_{{\rm in},m} \simeq R_m V_{Am}$.

Writing Eqs. (2) and (3) as functions of $\Delta z/\Delta x$ and substituting into Eq. (4) gives the predicted local rate. In the nonrelativistic limit ($\sigma_{x0} \ll 1$), the rate is

$$R_{0,NR} \simeq \frac{\Delta z}{\Delta x}\left(\frac{1-(\Delta z/\Delta x)^2}{1+(\Delta z/\Delta x)^2}\right)^2\sqrt{1-\left(\frac{\Delta z}{\Delta x}\right)^2}, \quad (5)$$

which is plotted as the solid curve in Fig. 2(a). This expression generalizes the previously known result [11,12,46] of $R_{0,NR} \simeq \Delta z/\Delta x \simeq \delta/L$ for small opening angles. In the $\Delta z/\Delta x \to 0$ and $\Delta z/\Delta x \to 1$ limits, $R_{0,NR}$ vanishes. Between the two extremes, $R_{0,NR}$ has a maximum, conforming to the discussion earlier. The maximum occurs at $\Delta z/\Delta x \simeq 0.31$ corresponding to a rate of 0.2, close to the fast rate of order 0.1 widely observed. More importantly, the local rate is relatively flat for a broad range of $\Delta z/\Delta x$ around the optimal value, suggesting that the rate is not strongly sensitive to the opening angle for intermediate values. This may explain why reconnection rates in disparate physical systems are so similar.

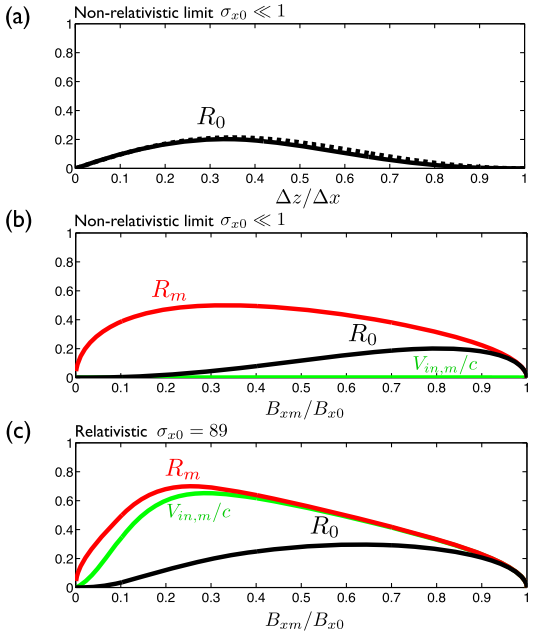

FIG. 2. Predictions for the nonrelativistic limit as functions of (a) $\Delta z/\Delta x$ and (b) B_{xm}/B_{x0}. (c) Predictions for relativistic limit ($\sigma_{x0} = 89$).

The dotted curve in Fig. 2(a) shows the nonrelativistic prediction if $V_{{\rm out},m}$ is taken to be identically V_{Am} in Eq. (4). This comparison indicates that the correction to the outflow speed in Eq. (3) does not significantly alter R_0, although it does impact R_m as $\Delta z/\Delta x$ approaches 1. Thus, the most significant effect limiting the *local* rate with an increasing opening angle is the embedding. We plot R_0, R_m, and $V_{{\rm in},m}/c$ in Fig. 2(b) as functions of B_{xm}/B_{x0} to facilitate a comparison with simulations. A similar plot is shown in Fig. 2(c) for the relativistic limit, specifically with $\sigma_{x0} = 89$. The peak R_0 is 0.3, and it does not change with increasing σ_{x0}. This bounds rates seen in relativistic simulations [45,50–53].

We point out that there are similarities between the present model and the classical Petschek model [14]. However, there are a number of important differences. For example, the Petschek model assumes a value of 0.5 for what we call B_{xm}/B_{x0}, whereas we estimate it self-consistently. Furthermore, the way Petschek obtained the upstream condition, strictly speaking, only works for the small opening angle limit, while our result is valid for any

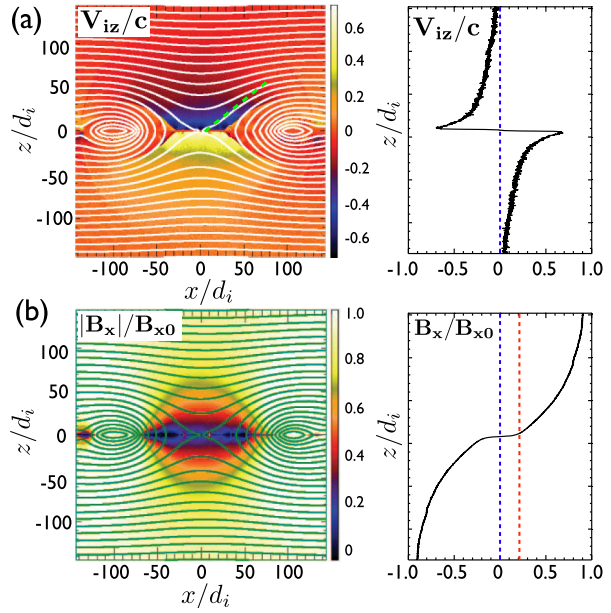

FIG. 3. Local-scale structure around the X line in electron-positron reconnection with $\sigma_{x0} = 89$ at $t = 600/\omega_{pi}$. (a) V_{iz} and its cut at $x = 0$. (b) $|B_x|$ and a cut of B_x at $x = 0$. The amplitude of B_{xm} is marked by the red dashed line, where the frozen-in condition $E_y + (\mathbf{V}_i \times \mathbf{B})_y/c = 0$ is violated. Contours of in-plane magnetic flux are overlaid. The color table in (b) has an upper limit B_{x0}.

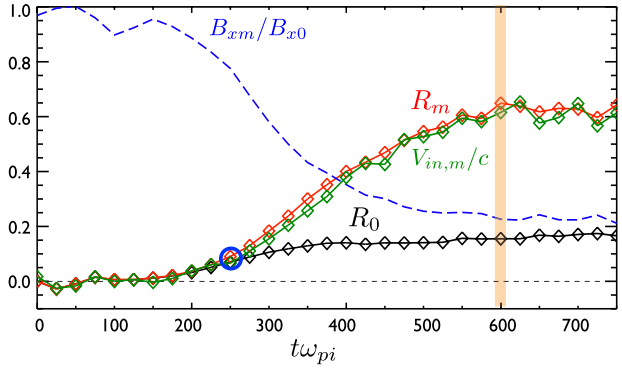

FIG. 4. Time evolution of the measured local reconnection rate R_0, microscale rate R_m, microscale inflow speed $V_{\mathrm{in},m}/c$ and B_{xm}/B_{x0}. The blue circle marks the deviation of R_m from R_0. The orange vertical line marks the time plotted in Fig. 3.

opening angle. Finally, and most importantly, the weak dependence on the reconnection rate reported by Petschek has a logarithmic dependence on the Lundquist number, so the normalized reconnection rate is not bounded by 0 and 1 as it must be on physical grounds. In the present work, the reconnection rate is manifestly bounded between 0 and 1.

Comparison to particle-in-cell simulations.—We compare the predictions against PIC simulations of a relativistic electron-positron plasma (i.e., $m_i = m_e$) in Ref. [45]. The upstream magnetization parameter $\sigma_{x0} = 89$ and $\beta = 0.005$. The diffusion region is embedded, as is clearly seen in Fig. 3, which shows the inflow velocity V_{iz} and reconnecting magnetic field B_x with in-plane magnetic flux overlaid at time $t = 600/\omega_{pi}$. A vertical cut through the X line of these quantities is also shown. Immediately upstream of the diffusion region of d_i-scale thickness, $|V_{iz}|$ peaks at $\simeq 0.65c$ and $|B_x|/B_{x0}$ drops to $\simeq 0.2$ ($d_i = c/\omega_{pi}$ is the ion inertial scale). The variation of the magnetic structure extends $\gtrsim 100 d_i$ upstream, and the separatrix has an opening angle wider than typically seen in the nonrelativistic regime with $\beta \sim O(1)$ (e.g., Ref. [18]). It was shown in Ref. [45] that the magnetic pressure gradient balances magnetic tension in the upstream region, as expected for this low-β system.

The time evolution of reconnection rates are plotted in Fig. 4, along with the microscale inflow speed $V_{\mathrm{in},m}$ and the ratio of magnetic fields B_{xm}/B_{x0}. Before a quasisteady state is reached, both R_m and R_0 increase as the simulation progresses. The deviation of R_m from R_0 occurs at time $t \simeq 250/\omega_{pi}$ and $B_{xm}/B_{x0} \simeq 0.8$. R_0 reaches a plateau of $\simeq 0.15$ at $t \gtrsim 300/\omega_{pi}$ while R_m continues to grow and B_{xm}/B_{x0} continues to drop. Note that, $R_0 \simeq 0.15$ is reached before the generation of secondary tearing modes at $t \simeq 500/\omega_{pi}$, indicating that R_0 is not determined by secondary islands. R_m eventually reaches a plateau of $\simeq 0.6$ and B_{xm}/B_{x0} drops to $\simeq 0.22$ at $t \gtrsim 600/\omega_{pi}$. The inflow speed $V_{\mathrm{in},m}$ traces R_m because $V_{Am} \simeq c$. We compare the steady-state values to the prediction shown in Fig. 2(c). Substituting the measured $B_{xm}/B_{x0} \simeq 0.22$ into the predictions gives $R_0 \simeq 0.14$, $R_m \simeq 0.69$, $V_{in,m} \simeq 0.62c$, and an opening angle $\theta \simeq 38.7°$ [illustrated by the dashed green line in Fig. 3(a)]. Given the simplicity of this model, this agreement is quite remarkable.

To test the predictions against nonrelativistic electron-proton reconnection, we compare with a low-β PIC simulation in Ref. [54], which used $m_i/m_e = 25$ and a background density 1% of the sheet density. The upstream $\beta = 0.01$. From that reference, $R_0 \simeq 0.085$ and $R_m \simeq 0.22$ with $B_{xm}/B_{x0} \simeq 0.55$. The predictions in Fig. 2(b) based on $B_{xm}/B_{x0} \simeq 0.55$ are roughly twice these values, mainly because of an overestimation of the outflow speed. However, it is common for electron-proton plasmas to have outflow speeds about half of the Alfvén speed [54]; this is likely due to a self-generated firehose-sense temperature anisotropy in reconnection exhausts, which reduces the outflow speed (e.g., Refs. [55,56]) but is not considered in the current model. Adjusting for this factor of 2, the predictions agree quite well with the simulations. The predicted opening angle ~28.8° purely based on the upstream constraint in Eq. (2) agrees well.

Discussion.—The model presented here is completely independent of the dissipation mechanism. The only ingredients are MHD-scale considerations and that the diffusion region remains at microscales when the opening angle increases. The fact that the simulated fast rates in disparate physical models are all similar to the predicted

maximum rate of order 0.1 suggests that MHD-scale constraints on magnetic energy release determine the fast rate. The obvious counterpoint to this is reconnection in MHD simulations with a uniform resistivity, which does not proceed at this rate. Even when the Lundquist number is large enough to produce magnetic islands [15,57], the reconnection rate is an order of magnitude smaller [58–60]. This indicates that considerations at MHD scales are not sufficient to explain fast reconnection; the microscale dissipation or localization mechanism must be able to support the desired opening angle at the local scale. However, if the diffusion region can support a larger opening angle, the local rate of order $\sim O(0.1)$ is not strongly sensitive to the opening angle over a wide range of values. The microscale rate R_m is sensitive to the opening angle, resulting in the large difference between R_m and R_0 observed in the relativistic limit [45].

The present model is not complete in that it does not include some physics that may affect the reconnection rate. As discussed earlier, the self-generated pressure anisotropy in the exhaust can reduce the outflow speed [55,56]. The plasma pressure gradient force in the outflow direction can also affect the outflow speed [26,54,61]. Self-generated upstream temperature anisotropies [62] may modify the embedding. Relaxing the low-β assumption is important. However, we note that the reduction of B_{xm} also occurs in simulations with $\beta \sim O(1)$ in Ref. [54]. This model does not take into account the conversion of upstream energy into heat and accelerated particles, which undoubtedly impacts the energy conversion process and is important in maintaining the intense current sheet during reconnection [46,63]. It also did not include the presence of an out-of-plane (guide) magnetic field, which will be the topic of future study. Finally, while this model is likely to apply to 3D reconnection that is quasi 2D, we do not take fully 3D systems or localized reconnection into account. Nevertheless, this simple model offers a new approach to the long-standing fast reconnection rate problem, which is broadly relevant in basic plasma physics, fusion science, solar and space physics, and astrophysics, and potentially provides an avenue for understanding the important link between the micro- and global scales.

Y.-H. L. thanks M. Swisdak and J. C. Dorelli for helpful discussions, and P. Wu and I. Honkonen for sharing their simulation data. Y.-H. L. is supported by NASA Grant No. NNX16AG75G. M. H. acknowledges support by NASA's MMS mission. F. G. is supported by NASA Grant No. NNH16AC601. H. L. is supported by the DOE through the LDRD program at LANL and DOE/OFES support to LANL in collaboration with CMSO. P. A. C. acknowledges support from NSF Grants No. AGS-0953463 and No. AGS-1460037 and NASA Grants No. NNX16 AF75G and No. NNX16AG76G. M. S. is supported by NSF Grant No. AGS-1219382. Simulations were performed with LANL institutional computing, NASA Advanced Supercomputing and NERSC Advanced Supercomputing.

[1] S. Masuda, T. Kosugi, H. Hara, S. Tsuneta, and Y. Ogawara, Nature (London) **371**, 495 (1994).
[2] R. E. Gershberg, *Solar-Type Activity in Main-Sequence Stars* (Springer, Berlin, 2005).
[3] J. A. Klimchuk, Phil. Trans. R. Soc. A **373**, 20140256 (2015).
[4] L. Kepko, R. L. McPherron, O. Amm, S. Apatenkov, W. Baumjohann, J. Birn, M. Lester, R. Nakamura, T. I. Pulkkinen, and V. Sergeev, Space Sci Rev **190**, 1 (2015).
[5] V. M. Vasyliunas, *Plasma Distribution and Flow*, edited by A. J. Dessler (Cambridge University Press, Cambridge, England, 1983), Chap. 395.
[6] M. Yamada, F. M. Levinton, N. Pomphrey, R. Budny, J. Manickam, and Y. Nagayama, Phys. Plasmas **1**, 3269 (1994).
[7] M. Yamada, Y. Ren, H. Ji, J. Breslau, S. Gerhardt, R. Kulsrud, and A. Kuritsyn, Phys. Plasmas **13**, 052119 (2006).
[8] L. Sironi, M. Petropoulou, and D. Giannios, Mon. Not. R. Astron. Soc. **450**, 183 (2015).
[9] E. G. Zweibel and M. Yamada, Annu. Rev. Astron. Astrophys. **47**, 291 (2009).
[10] E. N. Parker, Astrophys. J. **180**, 247 (1973).
[11] P. A. Sweet, in *IAU Symposium in Electromagnetic Phenomena in Cosmical Physics*, edited by B. Lehnet (Cambridge University Press, New York, 1958), p. 123.
[12] E. N. Parker, J. Geophys. Res. **62**, 509 (1957).
[13] E. N. Parker, Astrophys. J. **8**, 177 (1963).
[14] H. E. Petschek, Magnetic field annihilation, in *Proceedings of the AAS-NASA Symposium Physics Solar Flares* (1964), Vol. 50 of *NASA-SP*, p. 425.
[15] D. Biskamp, Phys. Fluids **29**, 1520 (1986).
[16] T. Sato and T. Hayashi, Phys. Fluids **22**, 1189 (1979).
[17] M. A. Shay, J. F. Drake, B. N. Rogers, and R. E. Denton, Geophys. Res. Lett. **26**, 2163 (1999).
[18] M. A. Shay and J. F. Drake, Geophys. Res. Lett. **25**, 3759 (1998).
[19] M. Hesse, K. Schindler, J. Birn, and M. Kuznetsova, Phys. Plasmas **6**, 1781 (1999).
[20] J. Birn, J. F. Drake, M. A. Shay, B. N. Rogers, R. E. Denton, M. Hesse, M. Kuznetsova, Z. W. Ma, A. Bhattacharjee, A. Otto *et al.*, J. Geophys. Res. **106**, 3715 (2001).
[21] B. N. Rogers, R. E. Denton, J. F. Drake, and M. A. Shay, Phys. Rev. Lett. **87**, 195004 (2001).
[22] J. F. Drake, M. A. Shay, and M. Swisdak, Phys. Plasmas **15**, 042306 (2008).
[23] N. Bessho and A. Bhattacharjee, Phys. Rev. Lett. **95**, 245001 (2005).
[24] W. Daughton and H. Karimabadi, Phys. Plasmas **14**, 072303 (2007).
[25] M. Swisdak, Y.-H. Liu, and J. F. Drake, Astrophys. J. **680**, 999 (2008).
[26] Y.-H. Liu, W. Daughton, H. Karimabadi, H. Li, and S. P. Gary, Phys. Plasmas **21**, 022113 (2014).
[27] J. M. TenBarge, W. Daughton, H. Karimabadi, G. G. Howes, and W. Dorland, Phys. Plasmas **21**, 020708 (2014).
[28] A. Stanier, A. N. Simakov, L. Chacoń, and W. Daughton, Phys. Plasmas **22**, 010701 (2015).
[29] P. A. Cassak, R. N. Baylor, R. L. Fermo, M. T. Beidler, M. A. Shay, M. Swisdak, J. F. Drake, and H. Karimabadi, Phys. Plasmas **22**, 020705 (2015).

[30] A. Stanier, A. N. Simakov, L. Chacoń, and W. Daughton, Phys. Plasmas **22**, 101203 (2015).
[31] G. T. Blanchard, L. R. Lyons, O. de la Beaujardière, R. A. Doe, and M. Mendillo, J. Geophys. Res. **101**, 15265 (1996).
[32] S. Wang, L. Kistler, C. G. Mouikis, and S. Petrinec, J. Geophys. Res. **120**, 6386 (2015).
[33] J. Qiu, J. Lee, D. E. Gary, and H. Wang, Astrophys. J. **565**, 1335 (2002).
[34] J. Lin, Y.-K. Ko, L. Sui, J. C. Raymond, G. A. Stenborg, Y. Jiang, S. Zhao, and S. Mancuso, Astrophys. J. **622**, 1251 (2005).
[35] H. Isobe, H. Takasaki, and K. Shibata, Astrophys. J. **632**, 1184 (2005).
[36] M. Ohyama and K. Shibata, Astrophys. J. **499**, 934 (1998).
[37] T. Yokoyama, K. Akita, T. Morimoto, K. Inoue, and J. Newmark, Astrophys. J. **546**, L69 (2001).
[38] H. Karimabadi, J. Dorelli, V. Roytershteyn, W. Daughton, and L. Chacón, Phys. Rev. Lett. **107**, 025002 (2011).
[39] A. Stanier, W. Daughton, L. Chacón, H. Karimabadi, J. Ng, Y.-M. Huang, A. Hakim, and A. Bhattacharjee, Phys. Rev. Lett. **115**, 175004 (2015).
[40] J. Ng, Y.-M. Huang, A. Hakim, A. Bhattacharjee, A. Stanier, W. Daughton, L. Wang, and K. Germaschewski, Phys. Plasmas **22**, 112104 (2015).
[41] L. Comisso and A. Bhattacharjee, J. Plasma Phys. **82**, 595820601 (2016).
[42] M. A. Shay, J. F. Drake, M. Swisdak, and B. N. Rogers, Phys. Plasmas **11**, 2199 (2004).
[43] E. R. Priest and T. G. Forbes, J. Geophys. Res. **91**, 5579 (1986).
[44] P. A. Cassak and J. F. Drake, Astrophys. J. **707**, L158 (2009).
[45] Y.-H. Liu, F. Guo, W. Daughton, H. Li, and M. Hesse, Phys. Rev. Lett. **114**, 095002 (2015).
[46] M. Hesse, S. Zenitani, M. Kuznetsova, and A. Klimas, Phys. Plasmas **16**, 102106 (2009).
[47] M. Hesse and S. Zenitani, Phys. Plasmas **14**, 112102 (2007).
[48] J. Birn, J. E. Borovsky, M. Hesse, and K. Schindler, Phys. Plasmas **17**, 052108 (2010).
[49] J. Sakai and T. Kawata, J. Phys. Soc. Jpn. **49**, 747 (1980).
[50] L. Sironi, D. Giannios, and M. Petropoulou, Mon. Not. R. Astron. Soc. **462**, 48 (2016).
[51] F. Guo, Y.-H. Liu, W. Daughton, and H. Li, Astrophys. J. **806**, 167 (2015).
[52] N. Bessho and A. Bhattacharjee, Astrophys. J. **750**, 129 (2012).
[53] M. Melzani, R. Walder, D. Folini, C. Winisdoerfer, and J. M. Favre, Astron. Astrophys. **570**, A111 (2014).
[54] P. Wu, M. A. Shay, T. D. Phan, M. Oieroset, and M. Oka, Phys. Plasmas **18**, 111204 (2011).
[55] Y.-H. Liu, J. F. Drake, and M. Swisdak, Phys. Plasmas **19**, 022110 (2012).
[56] Y.-H. Liu, J. F. Drake, and M. Swisdak, Phys. Plasmas **18**, 092102 (2011).
[57] N. F. Loureiro, A. A. Schekochihin, and S. C. Cowley, Phys. Plasmas **14**, 100703 (2007).
[58] W. Daughton, V. Roytershteyn, B. J. Albright, H. Karimabadi, L. Yin, and K. J. Bowers, Phys. Rev. Lett. **103**, 065004 (2009).
[59] Y.-M. Huang and A. Bhattacharjee, Phys. Plasmas **17**, 062104 (2010).
[60] L. S. Shepherd and P. A. Cassak, Phys. Rev. Lett. **105**, 015004 (2010).
[61] E. R. Priest and T. R. Forbes, *Magnetic Reconnection* (Cambridge University Press, Cambridge, England, 2000), Chap. 4.2.1, p. 121.
[62] J. Egedal, A. Le, and W. Daughton, Phys. Plasmas **20**, 061201 (2013).
[63] M. Hesse, T. Neukirch, K. Schindler, M. Kuznetsova, and S. Zenitani, Space Sci. Rev. **160**, 3 (2011).